REPORT DOCUMENTATION PAGE

AFRL-SR-BL-TR-00-

0354

8

1. AGENCY USE ONLY *(Leave blank)*	2. REPORT DATE	3. REPOR. TYPE AND DATES
		Final 01 Apr 97 - 31 Mar 00

4. TITLE AND SUBTITLE
Electrooptical Effects on Thin Organic Films and X-Ray Diffraction Analysis of 3-Nitroaniline and 2-Cyclo-Octylamino-5-nitropyridine

5. FUNDING NUMBERS
F49620-97-1-0256

6. AUTHOR(S)
Dr Alexander Leyderman/M. Antipin

7. PERFORMING ORGANIZATION NAME(S) AND ADDRESS(ES)
New Mexico Highlands University
National Avenue
Las Vegas NM 87701

8. PERFORMING ORGANIZATION REPORT NUMBER

9. SPONSORING/MONITORING AGENCY NAME(S) AND ADDRESS(ES)
AFOSR/NL
801 N. Randolph St.,Rm 732
Arlington VA 22203-1977

10. SPONSORING/MONITORING AGENCY REPORT NUMBER

11. SUPPLEMENTARY NOTES

12a. DISTRIBUTION AVAILABILITY STATEMENT
Approved for Public Release: Distribution Unlimited

12b. DISTRIBUTION CODE

13. ABSTRACT *(Maximum 200 words)*

During 3 years of AFOSR support, we have studied nonlinear properties of organic materials, their application for nonlinear device fabrications. In particular, we have studied a number of organic compounds, such as a conventional compound meta-nitroaniline, and a few compounds, which readily convert into a glass form. We give a brief description of our findings in the complete report.

20000718 093

14. SUBJECT TERMS
Electro-Optical, Organic Crystal Films,

15. NUMBER OF PAGES
12

16. PRICE CODE

17. SECURITY CLASSIFICATION OF REPORT	18. SECURITY CLASSIFICATION OF THIS PAGE	19. SECURITY CLASSIFICATION OF ABSTRACT	20. LIMITATION OF ABSTRACT
UNCLASS	UNCLASS	UNCLASS	

Final Technical Report to AFOSR Project F49620-97-1-0256

Electro-optical effects in thin single organic crystal films and x-ray diffraction analysis of 3-nitroaniline and 2-cyclo-octylamino-5-nitropyridine

by

Principal Investigator - Alexander Leyderman

Co- Principal Investigator - Mikhail Antipin

SUMMARY

During 3 years of AFOSR support, we have studied nonlinear properties of organic materials , their application for nonlinear device fabrications. In particular, we have studied a number of organic compounds, such as a conventional compound meta-nitroaniline, and a few compounds, which readily convert into a glass form. In the following, we give a brief description of our findings.

1. We have developed a method of fabrication of electro-optical device (Pockel's and Kerr cells), in which the crystal is well protected against damaging. A number of compounds has been studied and used for electro-optical cell fabrication, such as meta-nitroaniline (m-NA), and a few compounds, which readily convert into a glass form: 2-cyclo-octylamino-5-nitropyridine (COANP), N-(4-nitrophenyl)-(L)-prolinol (NPP), (S)-2-N-α-(methylbenzylamino)-5-nitropyridine (MBANP), 2-(N-prolinol)- 5-nitropyridine (PNP), 2-adamantylamino-5-nitropyridine (AANP), and numerous substituted derivatives of dicyanovinilbenzene (DIVA). These compounds revealed high values of nonlinear susceptibility, and our research efforts were concentrated on studies of nonlinear properties (SHG, electro-optical effects, Pockels and Kerr), differential scanning calorimetry, dielectric, ESR spectroscopy, and X-ray diffractometry for a number of single crystals of NLO-active compounds in order to understand and develop an approach to grow crystals of these compounds. Our devices demonstrate electro-optical effects under low voltage not exceeding 10 V. These studies inspired our further search for materials with large values of electro-optical coefficients and well defined cleavage planes.

2. Based on our method of thin crystal fabrication, we developed a method of light coupling into a waveguide using a prism conjugated with the electro-optical device. This project is in progress and supported by the BMDO Program, and the goal of it is to develop a miniature modulator with a crystalline film as a waveguide.

3. We have studied the calorimetry and dielectric properties of glasses and identified certain peculiarities of temperature and frequency dependence of permittivity. These studies are part of our efforts to understand the properties of organic and inorganic glasses. We have developed a multifractal approach in studies of phase transitions in glasses, relaxation time of which follows different pattern, either Cole-Cole's, or Davidson-Cole's, or Havriliak-Negami's. Our approach allows one to predict multifractal phase transitions based on studies of dielectric strength of glasses. This project is in progress.

4. Based on our findings, we studied the properties of a variety of sol-gel produced glasses to fabricate photosensitive devices. It was found that doped glass could be of interest for fabrication of quite stable photo-centers. Also, we have observed a peculiar phenomenon, in which some of our glasses revealed microwave (9 GHz) absorption saturation in magnetic field at low temperature (LN_2). This phenomenon has features of a superconductor and of a memory device. It is our understanding that it could be used by AFO in its efforts to protect the AFO aircrafts against detection by foe radars. We plan to send in the nearest future a proposal to the AFOSR to study this phenomenon and its application.

5. New accurate single crystal X-ray diffraction data including low-temperature ones were obtained for 2-cyclooctylamino-5-nitropyridine (COANP) and 2-adamantylamino-5-nitropyridine (AANP). COANP was found to form only one orthorhombic crystalline modification ($Pca2_1$, Z=4), and its structure at room temperature is characterized by a crystal disorder related to the flexibility of the cyclooctyl-ring. On the contrary, AANP forms two polymorph modifications which may be obtained from the melt or vapor phase ($Pna2_1$, Z=4), or by crystallization from acetonitrile solution (new $Pca2_1$-phase, Z=4). The last phase is

isostructural with COANP and is characterized by the optimal molecular orientation for highest effective NLO responses in the solid state. For both compounds molecular mechanics calculations of the molecular conformations have been performed together with calculations of the crystal packing and crystal morphology.

6. New low-temperature (120K) high-resolution X-ray diffraction data were obtained for the single crystal of meta-nitroaniline (mNA) in order to reveal some features of the electron density distribution responsible for NLO characteristics of this compound. New approach has been developed to estimate molecular and crystalline NLO responses directly from the X-ray diffraction data. This approach includes the use of new multipole program for refinement of the diffraction data and a new written program to estimate components of the β (or d) tensors directly from the multipole occupancies. The approach has been tested as well for the crystal of DIVA - dicyanovinylanizole (well known NLO material used as a standard), and new high-resolution diffraction data were obtained for this compound as well. Rather good agreement has been obtained between the estimated (from X-ray data) and measured NLO characteristics, which allows one to use the proposed approach for a prior estimation of NLO responses.

7. A large series of new organic chromophore compounds has been prepared and tested for NLO activity together with corresponding single crystal X-ray diffraction analysis of their molecular and crystal structure. Most of the compounds studied belongs to the series of substituted in the aromatic ring dicyanovinylbenzenes and substituted 4-aryl-1,1-dicyano-1,3-butadienes. Some of the compounds were found to possess quite large values of the molecular hyperpolarizability and some of them form acentric crystals. Among this series a several NLO-active compounds were suggested for further study and more detailed investigation as prominent NLO materials.

8. A special attention was paid to the study of polymorphism in organic NLO chromophore compounds similar to that found for COANP and AANP, and a several new polymorph modifications including NLO-active ones were found in the series of the compounds studied.

Part I - Nonlinear Properties of Organic Crystal films and Glasses

1-2. Electro-optical devices

The goal of this part of the project was: (i) to assemble the *dc* deposition system to obtain ITO transparent and conducting layer, which was successfully fulfilled, and (ii) to measure the electrooptical linear (Pockels) and quadratic (Kerr's) effects in cell fabricated from mNA, COANP, NPP, PNP, MBANP, AANP and others compounds. Our observations are published in a few papers [1-5].

Single crystal films with thickness of 5 to 20 μm were grown between two transparent fused quartz plates, on which indium-tin-oxide layers were deposited. Both linear and quadratic electro-optic effects of the crystals were examined by an *ac* modulation method. The figures of merit for mNA and COANP are estimated to be 3.2×10^{-12} m/V and 4.2×10^{-12} m/V, respectively. The crystals were of high quality due to the excellent protection provided by the cells and the figure of merits of all crystals did not decrease with time. It is believed that the method adopted is applicable to electro-optic cell fabrication with other compounds if those crystals grown from melt are feasible. It is suggested that the electro-optic cells have excellent potential use for device fabrication because of their durability and relative easy manipulation during crystal growth. Upon recommendation of Dr. Charles Lee of the AFOSR, we have tried to grow thin film of DUST compounds [6]. Unfortunately, we did not succeed because of its melt instability.

In co-operation with Dr. Sergey Sarkisov and his group of the A&M University at Normal, Alabama, we developed a method of crystalline film fabrication, which comprises our method of thin film growth with light coupling via a prism [5]. The method will allow one to use the advantage of high birefringence of organic material in wave guiding light. We have some technical problems to resolve in order to obtain a reliable and stable device comprising a light modulator with wave guiding.

3. Studies of glasses.

Some of compounds studied belong to organic glasses, and there was a challenge to grow from their melt crystalline films. We have studied the differential calorimetry (DSC) and the dielectric spectroscopy (DS) of some of these compounds [7, JPD 32], and found that COANP and NPP crystallizing

upon heating from glass state, while PNP [8] does not crystallize at all. Our studies revealed the crystallization point dependence on the rate of heating and/or cooling. The crystallization point is laying below melting point at least for 30 K. We also have found from DS measurements that the dielectric permittivity of the glass-like state of COANP drastically depends on the temperature distribution in the plane of the sample, and near the crystallization point a peculiarity in permittivity is observed. We proposed a model to explain this phenomenon and applying for a patent. We are looking for similar behavior in other glasses.

Our observations on glass properties, in particular, of the DC allowed us to propose a model of multifractal phase transitions based on analysis of the relaxation time pattern, characteristic of certain glass. We have analyzed [9,10] Debye, Cole-Cole, Davidson-Cole, and Havriliak-Negami patterns, and concluded that each of these patterns shows certain number of phase transitions, and the highest number of phase transitions (3) is obtained from Davidson-Cole pattern. The phases are characterized by the rates of relaxation. We continue to study the phase transitions in glasses. In continuing these studies our goal will be: (1) to evaluate the relaxation pattern based on non-extensive statistics, and (2) to show linkage between different patterns.

4. Photosensitivity of sol-gel produced TEOS and TEOS doped glasses [11].

The investigation of photosensitive materials has been an important subject in physics and material science due to their ability to store optical intensity distributions in the form of spatial pattern of altered refractive index. By exposing to irradiation, certain defects could be produced in the sample. These defects may contribute considerable influence on optical and electronic properties. Germanium doped SiO_2 glass has attracted much interest because it is used not only for a conventional optical fiber, but also for fiber-type function devices such as Bragg grating, which utilizes refractive-index change induced by the irradiation of UV photons [12-14]. Current understanding on photosensitivity in germania-silica system is associated with the presence of germanium and germanium-related defects. It has been reported that germanium related oxygen-deficient centers (GODCs) are responsible for the structure change, which causes the refractive-index change [15-17]. Different defect conversion processes could be reached under different irradiation condition [15,16], and could be examined by analyzing the change of UV absorption. Previous theoretical and experimental studies suggested that the formation and conversion of GODCs are correlated with the bleaching of 240 and 246 nm (5.1 eV band) absorption peaks. The photosensitivity, which results from the transformation of GODCs, is enhanced with the increase of optical bleaching at 5.1 eV absorption band [12,13,18].

Formation and conversion of GODCs might depend on the impurities contained in the sample as well as the irradiation condition and germanium concentration. The photosensitivity of the material could be changed by the variation of defect transformation process. Careful selected dopants such as aluminum, alkali ethoxides could affect the defect formation and transformation, and subsequently, influence the photosensitivity of the specimen [19]. To our knowledge, no such investigation has been reported in sol-gel TEOS synthesized glass systems. We concentrate our efforts on fabrication and studies of TEOS based sol-gel produced glasses, with dopants serving as source and acceptors of electrons [19]. The latter has to have a very high electron affinity to produce stable centers.

References:

1. A. Leyderman, Y. Cui. "Electro-optical characterization of 2-cyclo-octylamino-5-nitropyridine thin organic crystal film", *Optics Letter* **23,** 909-911 (1998).
2. A.Leyderman, Y. Cui, and B.G. Penn "Electro-optical effects in thin organic crystal films grown from melt" *J. Physics D: Applied Physics* **31** (20), 2711-2717 (1998).
3. A.Leyderman, Y. Cui. "Electro-optical effects in thin crystalline films of meta- nitroaniline and 2-cyclo-octylamino-5-nitropyridine" *SPIE* **3474,** *Proceedings of SPIE International*, 19-24 July, 1998, San Diego CA.
4. J. Wu Li, Y. Cui, and A.Leyderman,. "Pockels and Kerr's cells fabricated with thin organic crystal films" *Applications of photonic technology, SPIE Int.*, **3491**, 694-699 (1998).
5. A.Leyderman, Y.Cui, J.Wu, S.Sarkisov, M.Curley, Curtis Banks, Benjamin Penn "Growth and characterization of single crystal organic thin films for electro-optics modulators", *SPIE-99,* **3793,** 45-54 (1999).

6. Pan F., Knopfle G., Bosshard Ch., Follonier S., Spreiter R., Wong M.S., and Gunter P., *Appl. Phys. Lett.* **69**, 13 (1996).
7. Yunlong Cui, Javier Wu, Natalie Kamanina, Alfredo Pasaje, Alexander Leyderman, Alfonso Barrientos, Marcus Vlasse, and Benjamin Penn, "Dielectric study of dynamics of organic glasses" *Journal of Physics D: Applied Physics* **32** (24), 3215-3221 (1999).
8. Y. Cui, J.Wu, A. Leyderman, G.P.Sinha, F.M.Aliev, Dielectric spectroscopy study crystallization kinetics of N-(4-nitrophenyl)-(L)-prolinol glass, Submitted to *Journal of Physics D: Applied Physics.*
9. Shi-Xian Qu, Hirong Zheng, Alfonso Barrientos, Alexander Leyderman, "Multifractal Phase transitions in Davidson-Cole Relaxation Process", *Physics Letters A.* **268** (4-6), 360-365 (2000).
10. A. Leyderman, Shi-Xian Qu, "Multifractal phase transitions in non-Debye Relaxation Processes", Submitted to *Phys. Rev. E.*
11. A.Leyderman, H. Zheng, "Influence of Al ion on photochemical conversion in germania-silica xerogels", *J. of Luminescence* **83-84,** 447-451 (1999).
12. Kelly D. Simmons, George I Stegeman, Barrett G. Potter Jr and Joseph H. Simmons, *Journal of non-crystalline solids*, **179** (1994) 254.
13. Kelly D. Simmons, George I Stegeman, Barrett G. Potter Jr and Joseph H. Simmons, *Optics Letters,* **18** (1993) 25.
14. K.O.Hill, Y. Fujii, D.C. Johnso, and B.S.Kawasaki, *Appl. Phys. Lett.* **32** , 647 (1978).
15. Makoto Fujimaki,Kanta Yagi, Oshimichi Ohki, Hiroyuki Nishikawa, and Koichi Awazu, *Physical Review B*, **53**, 9859 (1996).
16. Hideo Hosono and Hiroshi Kawazoe and Junji Nishii, *Physical Review B*, **53,** R11 921 (1996) .
17. M. Josephine Yuen, *Applied Optics*, **21** 136 (1982).
18. D. L. Williams, S. T. Davey, R. Kashyap, J. R. Armitage and B. J. Ainsile, *Electronic Letters*, **28,** 369 (1992).
19. A.Leyderman, J.A.Weil and J.A.S.Williams, "Generation of Paramagnetic Centres in Crystalline Quartz by UV irradiation", *J.Phys.Chem.Solids* **46** (4), 519 (1985); A.Leyderman, J.A.Weil, P.C.Rao "Transformation of centers in alpha-quartz", unpublished.

Part II - X-Ray Structural Studies

1. X-Ray Diffraction Analysis of COANP and AANP.

In the present part of the Report results of the X-ray diffraction analysis of the molecular and crystal structures and polymorphism of COANP and AANP are presented. We directed our efforts to a search of new polymorph phases of these compounds using different techniques for crystal growth. We expected that polymorphism of COANP might be related to the conformational flexibility of the cyclooctane ring in this molecule. However, no new crystalline phases were found for this compound. The only manifestation of the molecular flexibility for COANP is probably the formation of a glassy state on cooling the melt, which results in a crystal structure disorder at room temperature[1]. To reveal the nature of this disorder (static or dynamic) we collected X-ray data for COANP at two temperatures 297 and 167K, respectively.

On the contrary, for the AANP we found two crystal phases, including one that was previously unknown. It was found that the $Pna2_1$-phase published earlier[2] may be obtained from the melt (see also[3]) as well as by a sublimation technique (present work). On the other hand, slow crystallization from acetonitrile solution results in formation of the new AANP phase (space group $Pca2_1$, Z=4) that is very similar and isostructural to the known COANP structure. So, AANP forms at least two non-centrosymmetric polymorph modifications having different crystal packing arrays. X-Ray diffraction analysis has been performed for both AANP phases obtained by sublimation ($Pna2_1$-phase, diffraction data were collected at room temperature) and by crystallization from acetonitrile solution (new $Pca2_1$-phase, data were obtained at room temperature and at 163K to increase accuracy of the diffraction data).

To understand details the of thermal behavior and polymorphism, we also performed molecular mechanics calculations of the molecular conformations and crystal packing energies for both compounds. These calculations were done to determine the factors which might be responsible for the glassy state of COANP, conformational polymorphism of AANP, and for determination of the more stable polymorph phase of AANP. Energetic calculations were also performed to evaluate crystal morphology of both compounds.

X-Ray Analysis. Single crystals of COANP and AANP (new $Pca2_1$-phase) suitable for X-ray analysis were obtained by slow crystallization from acetonitrile and had the shape of thin yellow prisms with the approximate dimensions 0.2x0.40x0.40 mm. The melting point of this phase for AANP was found to be 165°C. The $Pna2_1$-phase of AANP (thin plates) was obtained by slow sublimation in a sealed tube, these crystals have melting point 167°C. Unit cell parameters as well as the melting point of this phase were found to be identical with those for AANP crystal grown by zone melting.[2,3]

Unit cell parameters and intensities of reflections were measured with a 4-circle X-ray diffractometer "Siemens P3/PC" equipped with low temperature device (for COANP and $Pca2_1$-phase of AANP) and "CAD-4" diffractometer (for $Pna2_1$-phase of AANP) using MoKα radiation and θ/2θ-scan technique. Experimental details and results of refinements are summarized in **Table 1.** Experimental and calculations details are published in.[4]

Molecular mechanics, molecular packing and crystal morphology calculations. The molecular geometry of the COANP and AANP molecules was optimized using standard procedures and parameters incorporated in the MM3 program package. The dependence of the molecular conformational energy on the substituent orientation has also been calculated. Crystal packing calculations were carried out with the NONVPOT program package[5,6]. Lattice energy was calculated using the atom-atom approximation using different papameter sets. Computational evaluation of the crystal morphology has been performed with the same program package, using the known fact that crystal shape is determined by the relative rates of deposition of molecules on various faces.[7] The atom-atom potential method makes possible the calculation of the attachment (or adhesive) energy provided the crystal structure of the compound under investigation is known. As a rule, the most developed crystal faces are coplanar with the molecular layers having the highest intramolecular energy.

Molecular Geometry and Crystal Packing in COANP and AANP. Molecular geometry parameters are not unexceptional, nevertheless several features should be noted. In particular, a remarkable quinoid character in the pyridine ring bond length distribution was found in both structures. This may

indicate that the charge transfer direction mostly takes place along the N(2)...N(3) lines. Our quantum chemical AM1 calculations (MOPAC) have demonstrated that the dipole moment directions for the molecules are very close to these lines. Calculated values for the dipole moments were found to be 8.27D for COANP and 7.45D for AANP, respectively.

Crystal packing diagrams for COANP and AANP (for each of crystal phases) are presented in **Figure 1** in the projections more clear for their comparison. It is seen that for the COANP and AANP ($Pca2_1$) phases these diagrams are absolutely similar. Taking into account very close unit cell parameters for both compounds (Table 1) we may conclude that they are "isostructural". In these two crystals, molecules form endless "double" layers perpendicular to the longest ***a***-crystal axes and separated by the hydrophobic cyclooctyl- and adamantyl-substituents. So, the cleavage plane for these crystals most probably will be (100), i.e. the ***bc***-plane that was proven for COANP experimentally.[8] Along the polar ***c***-axes, the COANP and AANP molecules form infinite chains formed by the hydrogen bonds between the amino-nitrogen N(2) and the oxygen O(1') atom of the nitro-group.

The orientation of the molecular dipoles in the $Pca2_1$ phase for both COANP and AANP with respect to polar axes was found to be very close to the "optimal" value of 54.74° for efficient phase matching SHG for crystals with tmm2 symmetry. In particular, the angles between the polar crystal ***c***-axes and the molecular dipole moments are equal to 60.1° for COANP and 58.3° for AANP. The mutual orientation of the molecular dipoles has a herring-bone type with a relative shift of neighboring layers, so it may be defined more correctly as a "parquet-like" packing. Taking into account that both compounds have relatively high molecular second-order hyperpolarizabilities (calculated β values are equal to 33.9 and $34.3 \bullet 10^{-51}$ Cm^3V^{-2}, respectively for COANP and AANP; calculations were based on the X-ray geometry using the MOPAC and HYPER programs[9]), we may expect that the new $Pca2_1$-phase of AANP must possess quite large NLO-responses in the solid state.

Another type of crystal packing was found in the $Pna2_1$-phase of AANP (Figure 1). In this crystal, molecules also form layers along the polar ***c***-axis formed by the formation of the same type of N-H...O hydrogen bonds. The layers are separated by the adamantyl substituents and are perpendicular to the longest ***b***-crystal axis. The most important difference between the phases studied is the mutual orientation of the molecular dipoles along the polar crystal axes. In the $Pna2_1$-phase of AANP the dipoles form an "ideal" herring-bone array without relative shift of neighboring layers as was found in the $Pca2_1$-phases. Moreover, the angle between the AANP molecular dipole and the polar crystal axis in the $Pna2_1$-phase is equal to only 39.1°. Non-linear optical (SHG) properties of this phase (large single crystals were grown by a zone-melting technique) were first studied in[2] and it was established by the SHG measurements at 1064 nm that the d_{31} and d_{33} coefficients are rather large and equal to 80 and 60 pm/V, respectively, and therefore AANP was considered to be a very promising material for Type II angle-tuned phase-matched wavelength conversion with high efficiency in the optical communications wavelength region. We must note, however, that the authors[2] (see also[3]) were not aware that they were working with the "non-optimal" $Pna2_1$-phase of AANP, where the angle between the polar axis and charge transfer (molecular dipole moment) direction is equal to 39.1° only.

Molecular conformation calculations. As expected, the conformational behavior of COANP and AANP is different. Analysis of the cyclooctyl ring conformations shows that in all cases the ring conformation is the boat-chair (BC), that corresponds to that found in the crystal at both temperatures. The same conformation was indicated by several authors as corresponding to the lowest energy for the cyclooctane ring. In the gas phase coexistence of the two twist-chair-boat (TCB) and twist-boat-chair (TBC) conformations has been found for this flexible ring.[10] Our calculations also demonstrate that the orientational flexibility of COANP coexists with the ring flexibility. Both of these circumstances might be the reason for the formation of a glassy state by COANP on cooling the melt because of co-existence of many conformations in the melt having nearly the same energy, and crystal structure disorder at room temperature. Nevertheless, no new crystal phases were detected for COANP. At room temperature atomic thermal ellipsoids in COANP are very large indicating some kind of crystal disorder. On cooling the crystal, the ellipsoids size decreases almost linearly with the temperature, which might be an indication of the dynamic nature of the disorder related to the large flexibility of the cyclooctane ring.

Evaluation of the crystal morphology. In accord with our calculations (Table 2), in the crystals of COANP and AANP ($Pca2_1$-phases) the most developed faces are (100) and (-100) that are parallel to the molecular layers and perpendicular to the longest unit cell parameters. All other faces are less developed,

especially for the AANP crystal. As we noted before, this phase of AANP might posses rather large NLO responses because of optimal molecular orientation with respect to the more developed crystal face The situation somewhat differs from that for the AANP $Pna2_1$-phase where molecular layers are perpendicular to the crystal ***b***-axis. According to calculations, the more developed faces in this phase are perpendicular to the ***b***-axis and perpendicular to the ***c***-axis, as well as in the diagonal (110) direction. This result may indicate that a variation of the crystal growth conditions will allow one to obtain bulk crystals or thin films with different molecular orientations for desirable NLO applications. In particular, experimental EO measurements for COANP and AANP thin films are in a good agreement with these expectations.

Table 2. Relative surface areas for the most developed faces of COANP and AANP.

COANP		**AANP, $Pca2_1$**		**AANP, $Pna2_1$**	
Face index	Relative area	Face index	Relative area	Face index	Relative area
(100)	2.50	(100)	3.52	(010)	2.61
(011)	1.69	(110)	1.63	(001)	2.91
(110)	1.78	(101)	1.00	(00-1)	4.20
(10-1)	2.01	(10-1)	1.77	(110)	2.05
Crystal surface area	23.17		23.57		23.52

2. Electron Density Distribution in NLO Crystals.

The second goal of the project was related to the study of the electron density distribution in some NLO active crystals and direct estimation from these data molecular and crystalline NLO responses. Modern X-ray diffraction technique allows one to reconstruct an electron density distribution of crystals $\rho(\mathbf{r})$ and calculate directly many properties (atomic charges, dipole and higher multipole moments, electrostatic potentials, etc.) of molecules and crystals responsible for NLO activity. This is a way to a *prior* estimation of NLO characteristics of prospective materials in solid state, but until now there are only a few publications[11,12] where similar estimations have been done. Moreover, information about $\rho(\mathbf{r})$ will allow to describe the nature of chemical bonds and electron conjugation effects in NLO-active molecules in terms of their topological characteristics[13]. Modern approach in the $\rho(\mathbf{r})$ analysis in crystals is based on an *analytical presentation* of atomic densities by a sum over so-called pseudoatom non-spherical densities $\rho_{at}(\mathbf{r})$ centered at the nuclear positions ("multipole model"[14]).

While $\rho(\mathbf{r})$ may be presented in analytical form, it is possible to calculate form it some properties of atoms and molecules including those responsible for NLO characteristics, such as molecular dipole and higher moments. It is known that quadrupole and octupole moments of the molecular charge density are related to asymmetry of the π-electron clouds, and may be associated with components of the β-tensor. Multipole model allows one to determine the values of these moments via atomic multipole coefficients, and thus to estimate β values directly from the diffraction data. This new idea seems to be very prospective for *a prior* estimation of the NLO characteristics and it does not require the growth of large single crystals. The expression for the hyperpolarizability β via the components of the quadrupole and octupole moments Q_{xx} and T_{ijk} were obtained in[11,15]:

$$\beta_{ijk} = 4m^2/\hbar^4 \, T_{ijk} \, (Q_{ii} \, Q_{jj} + Q_{ii}Q_{kk} + Q_{jj}Q_{kk})$$

This expression was derived and used in our Project for calculation of the β tensor components from the molecular multipole moments obtained from diffraction data. Our estimations[12] for dicyanovinylanisole (DIVA) resulted in the value of β_{tot} equal to $15.1 \bullet 10^{-51}$ Cm^3 V^{-2} which is close to the experimental value ($18.7 \bullet 10^{-51}$) and quantum calculation ($12.35 \bullet 10^{-51}$). Similar estimation close to the measured data was performed as well for mNA crystal. Further development of this approach was related to calculation of the

crystalline NLO susceptibilities (*d*) for direct comparison with experimental data, and corresponding program has been written.

Figure 2 demonstrates experimental multipole and theoretical (6-31G**) deformation electron density maps (DED) in the molecular plane of DIVA together with the electrostatic potential map obtained as well from the multipole model. These data allowed one to formulate and understand the nature of chemical bonds and electron conjugation effects in this and similar molecules in terms of experimentally observed characteristics of the electron density[15] and create new structure/property relations.

3. Synthesis, Structural, and NLO Studies of New Organic Chromophores.

In the frame of the Project a large number (several dozens) of new potentially NLO active compounds were prepared and characterized by the single crystal X-ray diffraction data[17-21]. For most of them theoretical estimations of the molecular NLO responses were done and for some more prospective materials NLO measurements were also performed. One of the largest series of the compounds studied belongs to different derivatives of dicyanovinylaromatics and related compounds with longer electron conjugation chains. The combined X-ray, theoretical (calculations of NLO responses, molecular mechanics calculations of the molecular associates and crystal packing) and NLO study of this series allowed one to design a several new compounds having relatively large values of β, and forming acentric crystals. These compounds are rather active in SHG in solids; their formulae, space groups, measured and calculated β values ($10^{-51}Cm^3V^{-1}$) are listed below:

p-NMe_2-C_6H_4-CH=C(CN)$_2$	$P2_1$, Z=2	β_m=145.5,	β_c=88.6
o-F-C_6H_4-CH=C(CN)$_2$	Pc, Z=2	β_m=34.2,	β_c=10.2
p-Cl-C_6H_4-CH=C(CN)$_2$	$P2_1$, Z=2	β_m=46.4,	β_c=20.5
p-MeO-C_6H_4-CH=CH-CH=C(CN)$_2$	Pc, Z=2	β_m=103.5,	β_c=118.7

Good correlation was found between the predicted and experimental values of β in this series and different factors (molecular geometry, electronic nature and position of substituents in aromatic ring, the length of the conjugation path, the type of crystal packing array) influencing the magnitude of β were established. Some of these compounds (namely the fist and last ones shown above) may be recommended for application in NLO devices for second harmonic generation and electrooptics.

4. Search for New Polymorph Phases in NLO-Active Materials.

The final part of the Project was related to the further study of the polymorphism in organic NLO materials. This phenomenon might be very important for a search of new NLO-active acentric crystal modifications for a given chromophore compound. One of examples of such a polymorphism was considered earlier for AANP (see above). During the work on the Project we tried to crystallize systematically all prepared and potentially NLO active compounds under differing crystallization conditions and from different solvents, and in some cases new crystal phases were detected and studied. **Figure 3** demonstrates results of the study of derivative of 1,1-dicyano-1,3-butadiene, which forms at least two crystal phases. This compound has rather large value of the molecular hyperpolarizability and therefore might be used as a dopant in polymer matrices.

References.

1. Leyderman, A.; Espinosa, M.; Timofeeva, T.; Clark, R.; Frazier, D.; Penn B. *Proc. SPIE,* **1996**, *2809*, 144.
2. Tomary, S.; Matsumoto, S.; Kirihara, T.; Suzuki, H.; Ooba, N.; Kaino, T. *Appl. Phys. Lett.* **1991**, *58(23)*, 2583-2585.
3. Yokoo, A.; Tomaru, S.; Yokohama, I.; Itoh, H.; Kaino, T. *J. Cryst. Growth.* **1995**, *156*, 279-284.
4. Antipin, M.Yu.; Timofeeva, T.V.; Clark, R.D.; Nesterov, V.N.; Dolgushin, F.M.; Leyderman, A. *Chem. of Mater*, **2000**, submitted.

5. Shil'nikov, V.I. *Kristallografia.* **1994,** *39,* 647.
6. Timofeeva, T.V.; Shil'nikov, V.I.; Clark, R.D. *Proc. SPIE.* **1997,** *3123,* 159.
7. Hartman, P.; Bonnema, P. *J. Cryst. Growth.* **1980,** *49,* 157-165.
8. Günter, P.; Bosshard, Ch.; Sutter, K.; Arend, H. *Appl. Phys. Lett.* **1987,** *50(9),* 486-488.
9. Cardelino, B.H.; Moore, C.E.; Stuckel, R.E. *J. Phys. Chem.* **1991,** *95,* 8645-8652.
10. Dorofeeva, O.V.; Mastryukov, V.S.; Allinger, N.L; Almenningen, A. *J. Phys. Chem.***1990,** *94,* 8044.
11. Fkyerat, A.; Guelzim, A.; Baert, F.; Zyss, J.; Perigaud, A. *Phys. Rev.B.* 1996, **53,** 16236-16246.
12. Antipin, M.Yu.; Clark, R.D.; Nesterov, V.N.; Lyssenko, K.A., Timofeeva, T.V. *Proceedings of SPIE,* San Diego, California, **1998,** *vol. 3474,* 41-52.
13. R.F.W. Bader. *Atoms in Molecules: A Quantum Theory.* Oxford University Press, Oxford, U.K. **1991.**
14. Hansen, N.K.; Coppens, P. *Acta Crystallogr.A.* **1978,** *34,* 909-921.
15. Boyd, R.W. *Nonlinear Optics.* Academic, New York, **1992.**
16. Antipin, M.Yu.; Clark, R.D.; Nesterov, V.N.; Sanghadasa, M.; Timofeeva, T.V.; Lyssenko, K.A. *Mol. Cryst. Liq.Cryst.* **1998,** *313,* 85-94.
17. Antipin, M.Yu.; Barr T.A.; Cardelino B.H.; Clark R.D.; Moor C.E.; Myers T.; Penn B.; Sanghadasa M.; Timofeeva T.V. *J. Phys. Chem.B.* 1997, **101,** 2770-2781.
18. Antipin M.Yu.; Timofeeva, T.V.; Clark, R.D.; Nesterov, V.N.; Sanghadasa, M.; Barr, T.A.; Penn, B.; Romero, L.; Romero, L. *J. Phys. Chem. A.* **1998,** *102,* 7222-7232.
19. Nesterov, V.N.; Antipin, M. Yu.; Timofeeva, T.V.; Clark, R.D. *Acta Cryst. Ser. C,* **2000,** *C56,* 88-89.
20. Nesterov, V.N.; Timofeeva, T.V.; Borbulevych O. Ya.; Antipin, M. Yu.; Clark, R.D. *Acta Cryst. Ser. C,* **2000,** *C56,* in press.
21. Nesterov, V.N.; Kislyi, V.P.; Timofeeva, T.V.; Antipin, M. Yu.; Semenov, V.V. *Acta Cryst. Ser. C,* **2000,** *C56,* e107-e108.

Table 1. Structure Determination Summary for COANP and AANP ($Pca2_1$ and $Pna2_1$ phases)

	COANP (298K)	COANP (167K)	AANP (163K, $Pca2_1$)	AANP (298K, $Pca2_1$)	AANP (298K, Pr
empirical formula	$C_{13}H_{19}N_3O_2$	$C_{13}H_{19}N_3O_2$	$C_{15}H_{19}N_3O_2$	$C_{15}H_{19}N_3O_2$	$C_{15}H_{19}N_3($
formula weight	249.31	249.31	273.33	273.33	273.33
crystal size(mm)	0.2x0.4x0.4	0.2x0.4x0.4	0.2x0.3x0.4	0.2x0.3x0.4	0.2x0.2x0
space group	$Pca2_1$	$Pca2_1$	$Pca2_1$	$Pca2_1$	$Pna2_1$
Z	4	4	4	4	4
unit cell dimensions					
a, Å	26.285(5)	26.099(5)	28.158(6)	28.310(10)	7.991(2)
b, Å	6.647(1)	6.637(2)	6.584(2)	6.612(2)	26.326(6)
c, Å	7.631(2)	7.555(2)	7.395(1)	7.474(2)	6.588(1)
volume, $Å^3$	1333.3(5)	1308.7(6)	1371.0(5)	1398.9(7)	1385.9(5)
density (calc, g/cm^3)	1.242	1.265	1.324	1.298	1.310
abs. coeff. (cm^{-1})	0.86	0.87	0.90	0.88	0.89
F(000)	536	536	584	584	584
temperature,K	298(2)	167(2)	163(2)	298(2)	298(2)
θ range (deg)	3.06-27.57	1.56-27.55	1.45-40.09	1.44-27.05	2.66-24.9
scan range (ω, deg)	1.90	1.90	1.80	1.90	1.90
independent refls.	1657	1622	4242	1645	1322
obs. refls. ($I>2\sigma(I)$)	847	915	2919	565	329
no. of param. refined	163	163	257	185	181
final R_1 (obs. data)[1)]	0.0736	0.0592	0.0513	0.0719	0.0659
final wR_2 (all data)[2)]	0.2592	0.1637	0.1535	0.4079	0.2310
goodness of fit	1.068	1.021	1.022	1.008	0.863
Absolute structure param.[3)]	-1(5)	1(3)	0.9(13)	1(6)	5(5)
largest diff. peak ($e/Å^3$)	0.194	0.172	0.300	0.182	0.178
largest diff. hole ($e/Å^3$)	-0.189	-0.182	-0.243	-0.223	-0.148

[1)] $R_1 = \Sigma \| F_o - \| F_c \| \| / \Sigma(F_o)$

[2)] $wR_2 = \{\Sigma[w(F_o^2 - F_c^2)^2] / \Sigma w(F_o^2)^2\}^{1/2}$

[3)] Flack absolute structure parameter *x* (Flack, H. D. *Acta Crystallogr. A.* **1983**, A39, 876).

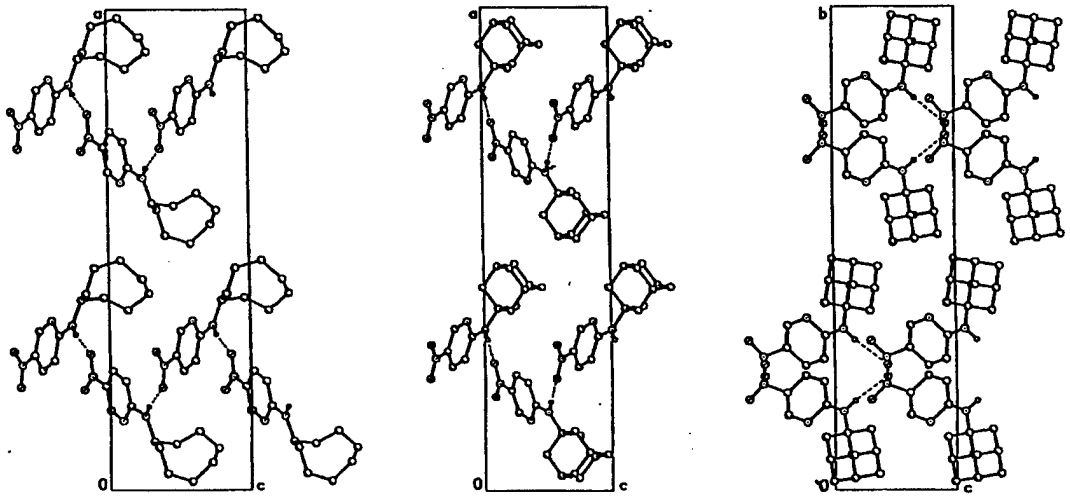

COANP
$Pca2_1$

AANP
$Pca2_1$

AANP
$Pna2_1$

Figure 1.

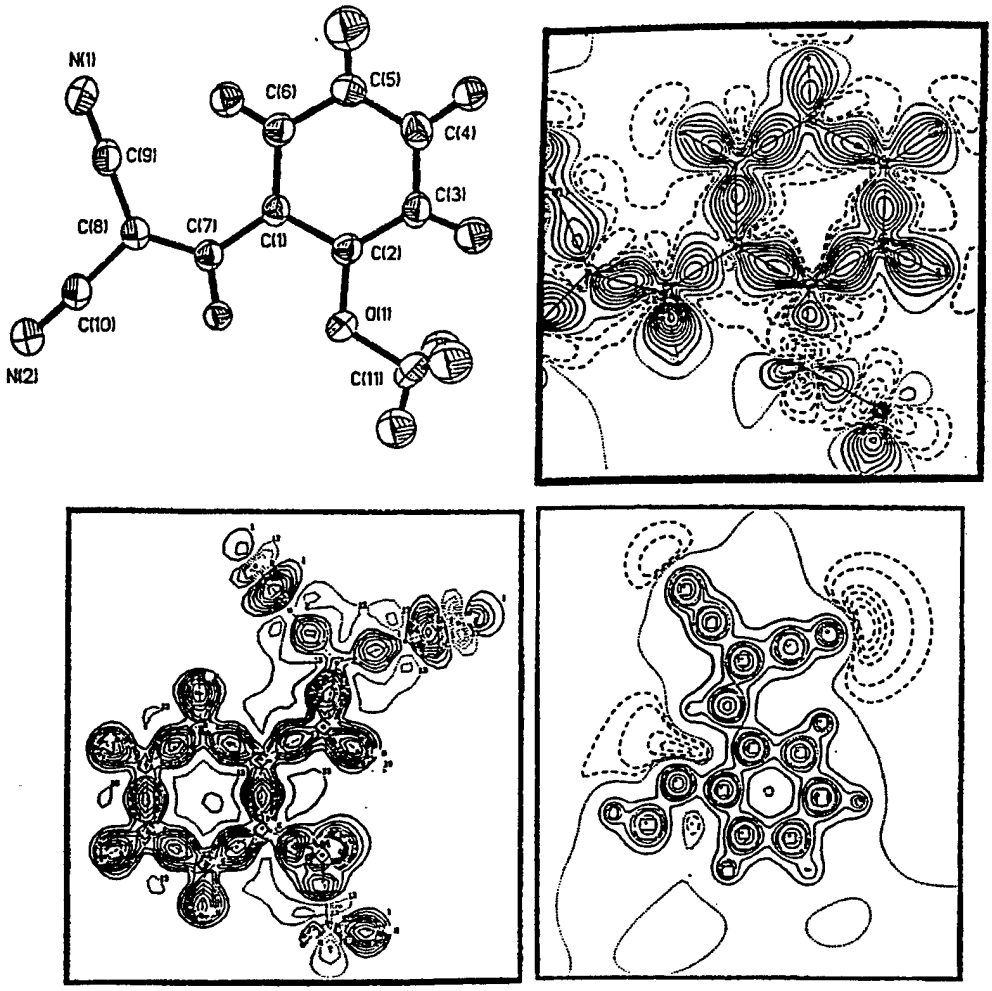

Molecular structure of DIVA (II), experimental multipole static DED map (top right, isolines are drawn through 0.1 e/Å^3), theoretically calculated DED map (6-31G** basis set, bottom left), and the map of the electrostatic potential (bottom right) in the mean molecular plane.

Figure 2.

Molecular structure and crystal packing for two modifications of 4-(4-dimethylaminophenyl)-1,1-dicyano-1,3-butadiene

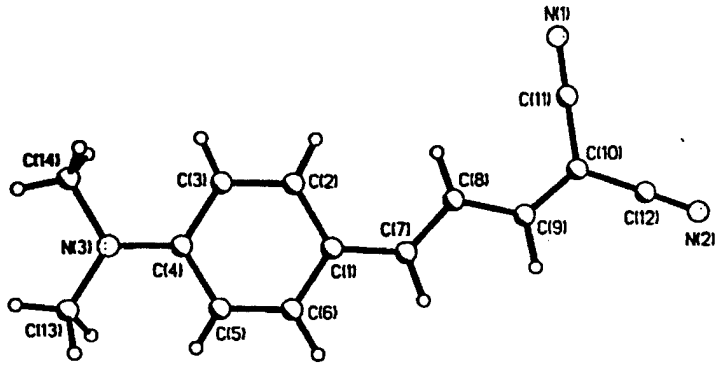

Red needles		Dark red bulk prisms	
a=7.091(1) Å	$P2_1/n$	a=10.060(2) Å	$P2_1/c$
b=11.425(2) Å	V=1229.6(4) $Å^3$	b=15.957(3) Å	V=1245.2(4) $Å^3$
c=15.423(3) Å	Z=4	c=7.938(2) Å	Z=4
β=100.24(3)°	D_{calc}=1.206 g/cm^3	β=102.26(3)°	D_{calc}=1.191 g/cm^3

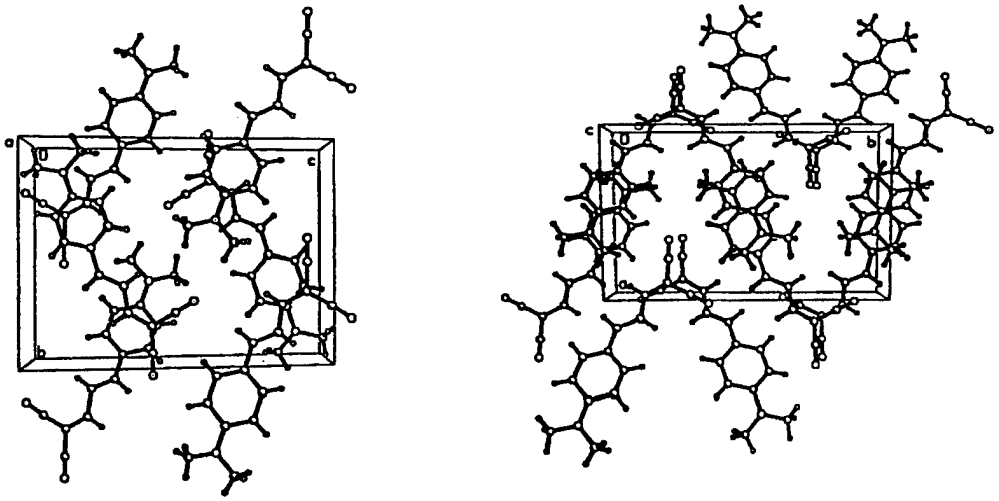

Figure 3.